Revue Roumaine de Chimie, **2007**, *52*(3), 235–241

SYNTHESIS AND OPTICAL PROPERTIES OF TiS_2 NANOCLUSTERS

Alexandru L. LET,* David MAINWAING, Colin RIX and Pandiyan MURUGARAJ

School of Applied Science, Science, Engineering and Technology Portfolio, Royal Melbourne Institute of Technology, GPO Box 2476V, Melbourne, Vic-3001, Australia

Received May 22, 2006

High-quality, nano-sized clusters of TiS_2 have been successfully grown inside inverse micellar cages and their optical properties studied. The clusters exhibit large blueshifts in the optical-absorption features with decreasing cluster size due to quantum confinement, affording control of the absorption thresholds and a demonstration of the crossover from band-like to molecule-like spectra as the size of the clusters becomes smaller than that of the exciton in the bulk.

INTRODUCTION

In its most common form, bulk titanium disulphide (TiS_2) crystallizes in a hexagonal layered structure ($P3\bar{m}1$) consisting of one hexagonally packed sheet of metal atoms contained between two hexagonal sheets of chalcogens for each layer, where atoms within a layer are bound by strong covalent forces.

This structural arrangement leads to metal atoms surrounded by six chalcogen atoms in an octahedral environment (Fig. 1), resulting in weak chalcogen-chalcogen van der Waals interactions between adjacent layers with S-Ti-S sandwiches stacked along the c axis. (c=5.6912 Å).[1]

Titanium disulfide possesses one of the highest intercalation energies when lithium diffuses into the van der Waal's gap between sulfur layers and most research has focused on its use as the cathode material in lithium rechargeable batteries. This has arisen from the need to produce portable power supplies; as the computer, medical and other devices become smaller, there is a need to produce smaller storage batteries to power them. Other applications include its use as a solid state lubricant in space-borne vehicles, as a hydrogenation catalyst [2], and as a possible hydrogen storage material.[3]

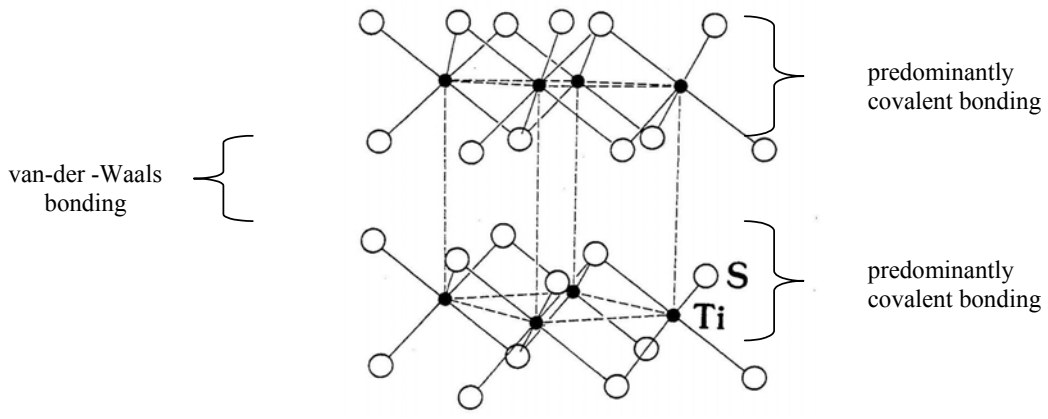

Fig. 1 – Structure of TiS_2.

* Corresponding author: alexandu.let@cap-xx.com

The bulk form of TiS_2 is optically opaque. Myron and Freeman[4] determined the electronic energy band structure of layered TiS_2 using the Korringa-Kohn-Rostoker (KKR) method and found it to behave as a semiconductor with a fundamental gap of 2.0 eV and a smaller indirect gap of 1.4 eV. The electronic spectrum of bulk TiS_2 has been studied extensively and consists of two main absorption bands between 0 and 3.5 eV.[5,6] The low energy band is centered around 2.3 eV with a width of 1.5 eV (as shown in Fig. 5, dotted line) and can be ascribed to electronic transitions from the upper p-bands into the lower triplet of non-bonding d-bands, followed by a window due to the separation between the lower non-bonding and the upper non-bonding d bands.

The optical and electronic properties of semiconductor nanoclusters have recently been studied experimentally and theoretically, especially in group II-VI semiconductors (CdS, CdSe, ZnS, ZnSe).[7] Much of this interest results from the potential application of nanoscale electronic and optical devices. Many of these applications exploit the fact that the properties of these materials can be quite different from those of bulk semiconductors.

Nano-size clusters are a special class of material which possess a variety of unique electronic and chemical properties as a consequence of quantum confinement, and their very large surface-to-volume ratios, and they are often referred to as "quantum dots" (QDs). The evolution of cluster properties with size is an important phenomenon, since the manifestation of electron and hole confinement gives way to discrete molecule-like electronic states as the cluster size decreases below the excitonic Bohr radius.

Quantum confinement results in the dense continua of valence and conduction band electronic states becoming discrete, well separated states and causes an increase in the band gap energy.[8-10] Thus, in nanometer sized semiconductor particles, the valence and conduction bands are replaced by manifolds of individual, delocalized electronic states. The energy shift of the band edge, as well as the separations between conduction and valence band states, can be larger than 1eV. In addition to these delocalized electronic states, semiconductor nanoclusters can also have localized electron and hole traps which often accumulate at the nanocluster surface, and the large surface to volume ratio can result in a high density of trap states. The presence of a high density of localized states along with finite relaxation rates between localized and delocalized states can affect the observed nanocluster optical properties.[11]

The preparation of such nanoparticles requires an appropriate "nanochemical reactor" in which to perform synthesis reactions, and this can be achieved using micelle structures, which are able to create a reaction template in the appropriate size range. It is well known that size control during colloidal growth requires the distinct separation of nucleation from growth. If nucleation occurs continuously, in either space or time, a wide range of cluster sizes will inevitably occur. However, if confinement of the reactant precursors can be achieved to limit growth to a restricted region of space, a narrow size distribution of clusters will occur.

Surfactant molecules can form segregated droplet-like aggregates called inverse micelles whose dimensions are typically 1-10 nm. The modifier "inverse" refers to the negative curvature between the surfactant-oil interface (the oil is the continuous medium). Nucleation only occurs in the micelle interior because of the total lack of solubility of charged species in the low dielectric constant inert oils used as the continuous medium.[12-13]

In this paper we report the synthesis of novel nano-sized clusters of titanium disulfide (TiS_2) using a synthetic strategy similar to that described previously for MoS_2 and WS_2 nanoclusters.[14-18] This represents the first reported room temperature synthesis of TiS_2 nanoparticles having a unimodal distribution of particle diameters in the range 3-5nm.

RESULTS

The nanoclusters were characterized by high resolution transmission electron microscopy (HRTEM) and optical spectroscopy. Figure 2 shows a HRTEM micrograph of TiS_2 clusters deposited on a carbon grid. The nanocluster images indicate they are very thin with irregular shapes and dimensions of about 3 to 6 nm. The darker images indicate that these particles are thicker and are believed to be aggregates. Some degree of aggregation is very difficult to avoid under the conditions of sample preparation.

It is difficult to obtain x-ray diffraction from such small clusters, but the electron diffraction patterns in the Fig.3 (a,b) shows that the clusters retain the bulk structure.

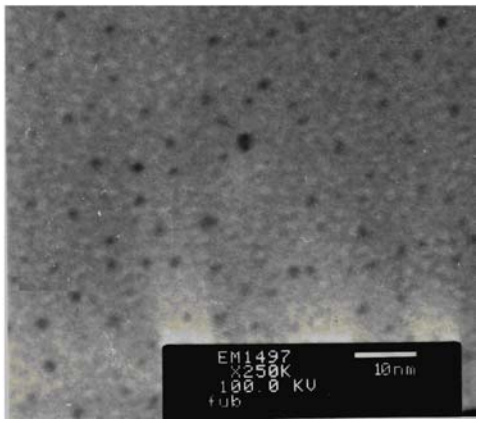

Fig. 2 – TEM image of TiS_2 nanoclusters having dimensions of approximately 2-5 nm.

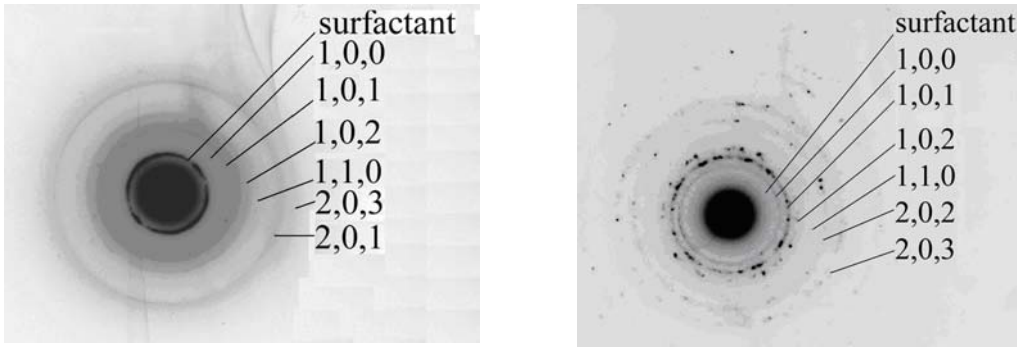

a b

Fig. 3 – Electron diffraction results taken from TiS_2 nanoclusters. a and b correspond to shorter and longer exposures respectively of the same sample.

The diffraction pattern shows continuous rings containing some discrete spots for short exposures and more discrete spots, rather than continuous rings, for longer exposures. This results from there being a finite number of nanoclusters or nanocluster aggregates on the irradiated surface. The electron diffraction results yield information regarding the nanocluster morphology. The reflections associated with only the c-axis, specifically the (0,0,1), (0,0,2), (0,0,3), (0,0,4) and (0,0,5) are absent in the observed electron diffraction pattern, which indicates that there is no long-range periodicity along the c-axis. The crystallographic c-axis is perpendicular to the planes associated with the S-Ti-S trilayers in bulk TiS_2, and so the electron diffraction pattern is consistent with the nanoclusters being two-dimensional, specifically consisting of a single, or only a few trilayers. The nanoclusters are expected to grow by the addition of Ti and S at the reactive trilayer edges. Growth along the c-axis corresponds to further nucleation and should therefore be relatively slow. This single trilayer morphology has been observed in images of MoS_2[17] and PtS_2[19] nanoclusters which also possess a layered crystal structure.

Table 1 also indicates that particle sizes calculated from the Debye-Scherrer expression change with the h,k,l refection used, indicating the lamella morphology of the TiS_2 nanoclusters. Generally, the lattice parameters showed a gradual increase with decreasing particle size as may be expected from lattice relaxation in nanosized crystallites, with the c_o parameter showing significant size dependence consistent with weak van der Waals forces along the c-axis.

Titanium sulfide nanoclusters in both octane and acetonitrile/TDAI/hexanol phases show nearly identical absorption spectra, with the lowest energy maxima at 359 nm. For comparison, the absorption spectrum of TiS_2 (bulk) and TiS_2 (nanoclusters) synthesized in ternary micelles and extracted into octane and acetonitrile are presented in Fig. 4, which illustrates the blue shift with decreasing size, and a cross-over from solid-like to molecular spectra of the small TiS_2 nanoclusters in acetonitrile.

Table 1

Calculated lattice parameters and particle sizes from the XRD, electron diffraction and HRTEM data on TiS_2 nanoparticles

XRD Reflections	FWHM	Particle Size (nm)	Lattice parameters (nm)	
			a_o	c_o
(1,0,1)	0.253	38.00	0.3405[a]	0.5612
(0,0,1)	0.163	40.57		
(1,0,1)	0.804	11.96	0.3405[a]	0.5692
(0,0,1)	0.471	15.21		
		3-5 (HRTEM)	0.3408*	0.5701*

* indicates the parameters are obtained from electron diffraction
[a] the parameters of the TiS_2 obtained by sol-gel[20]

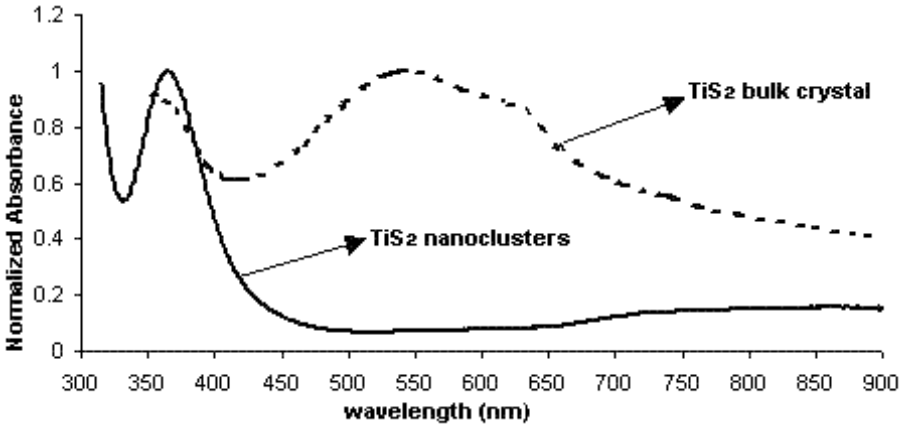

Fig. 4 – Absorption spectrum of small TiS_2 nanoclusters in octane compared with TiS_2 bulk[5].

DISCUSSION

Comparison of the spectrum of the clusters to that of the bulk crystal reveals a large blueshift for the clusters, and preservation of the excitonic features in the spectrum of the clusters. The TiS_2 nanoclusters studied should also have an indirect transition at lower energy but this transition is forbidden, and sufficiently weak that it is not observed in the absorption spectra. The first direct transition in the clusters spectrum occurs at λ = 359 nm (3.46 eV) which is associated with the excitonic peak of the bulk material at λ = 542 nm (2.29 eV), corresponding to a blueshift of 1.17 eV for the 3.0 nm clusters. This blue shift is a consequence of the quantum confinement of the electronic charge carriers in small clusters. The spacing between energy levels increases by decreasing the cluster size, and leads to an increase in the bandgap and shifts in the band edges.[21]

Because of the presence of I^- (from TDAI) during the synthesis, it was possible that the UV-visible peak was due to molecular species rather than nanoclusters, specifically I_3^- / I_5^-. Two results indicate that the peak is due to TiS_2 nanoclusters rather than I_3^- / I_5^-. First, the blank spectrum (synthesis, except without the $TiCl_4$) shows no absorbance at wavelengths > 290 nm in either the acetonitrile or octane phases. Secondly, I_3^- / I_5^- is insoluble in the octane phase. These results indicate that while it is possible to get spectral contamination in the acetonitrile phase, this does not occur in the octane phase and the absorption is due exclusively to TiS_2 nanoclusters. The introduction of a small amount of I_2 into the blank followed by extraction gives the I_3^- absorption peaks only in the acetonitrile phase since it is insoluble in the octane phase.

The blueshift of the first absorption peak in the nanocluster spectra may be qualitatively understood in terms of simple quantum confinement theory.[21-23] In this effective mass approximation theory, the energy shift of the first absorption peak in a quantum confined semiconductor is given by :

$$\Delta E = \frac{\hbar^2 \pi^2}{2R^2}\left[\frac{1}{m_e^*} + \frac{1}{m_h^*}\right] - \frac{1.8e^2}{\varepsilon R} + \textit{polarization terms} \quad (1)$$

where m_e^* and m_h^* are the electron and hole effective masses, respectively, ε is the dielectric constant, and R is the radius of the particle. This treatment assumes the particle to be spherical, and assumes that the motions of electron and hole may be described in terms of their effective masses. It also ignores the effect of surface atoms. The first and second terms on the right of Eq.1 are kinetic energy and electrostatic (Coulombic) attraction terms, respectively. The basic relationship between size and optical spectra was first developed and confirmed for ZnS and CdS nanoparticles. It is generally found that the kinetic energy term dominates, resulting in a blueshift in the absorption spectrum as the size of a nanocluster is decreased. In this simple treatment, as the cluster gets smaller, the band gap gets larger because the conduction band moves to more negative potentials, and the valence band moves to more positive potentials. The extent to which each band moves depends on the relative values of m_e^* and m_h^*. In most semiconductors, m_e^* is much less than m_h^*, so that most of the increase in the band gap is due to the conduction band moving to more negative potentials, the valence band moves very little.[22-25] If the bulk TiS_2 dielectric constant (13.7)[26] and typical electron (0.23 m_e)[27] and hole ($\sim m_e$) effective masses are used, then the Bohr radius may be estimated as being 2.5 nm.

Equation (1) may not be rigorously and quantitatively applied to the TiS_2 nanoclusters studied because the assumptions underlying the equation are rather poor approximations in this case, since the nanoparticles are certainly not spherical, as is assumed by Eq.1. Furthemore, the effective mass approximation, which is implicit in Eq.1 is derived from the periodic nature of the lattice. Nevertheless, Eq.1 can be used to provide qualitative insights into the size dependent properties of TiS_2 nanoclusters.

While the absorption spectra of these nanoclusters are the same in the octane and acetonitrile environments, the emission studies reveal some differences. The emission spectra of the TiS_2 nanoclusters in octane and acetonitrile, when λ_{exc}=312 nm, are compared in Fig. 5. The octane emission spectrum has a broad shoulder at around 430 nm and a peak centered at 450 nm, whereas the acetonitrile emission spectrum has a shoulder at 400 nm and a broad peak at 415 nm.

When excited at 360 nm, the spectrum of the TiS_2 clusters in octane exhibits an emission peak centered at 450 nm and the acetonitrile spectrum has a stronger peak at 400 nm accompanied by a broad and weaker peak at 415 nm.

In nanoclusters, a large number of the atoms are at or near the surface, leading to a preponderance of dangling bonds and defects, which result in surface states. Adsorbed impurities can also produce additional surface states and all these states can act as traps or recombination sites. The fate of photogenerated electron-hole pairs in a semiconductor is determined by traps and recombination processes.

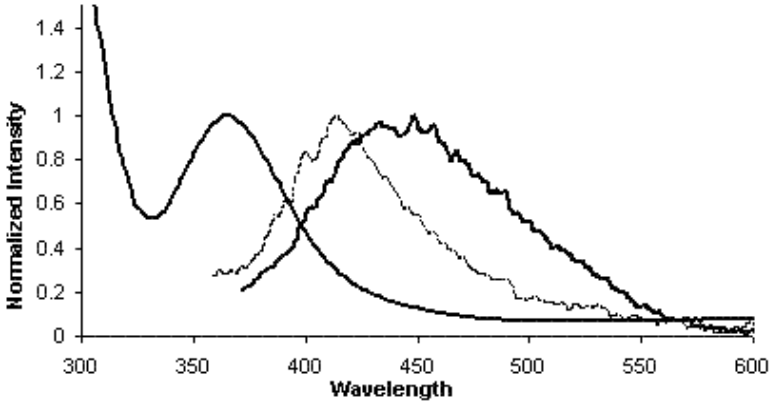

Fig. 5 – Absorption and emission spectra of TiS_2 nanoclusters. The absorption spectrum in octane (solid curve on left), emission spectrum in octane (solid curve on right) and the emission spectrum in acetonitrile (dotted curve) are shown for comparison. The emission spectra were excited at 312 nm.

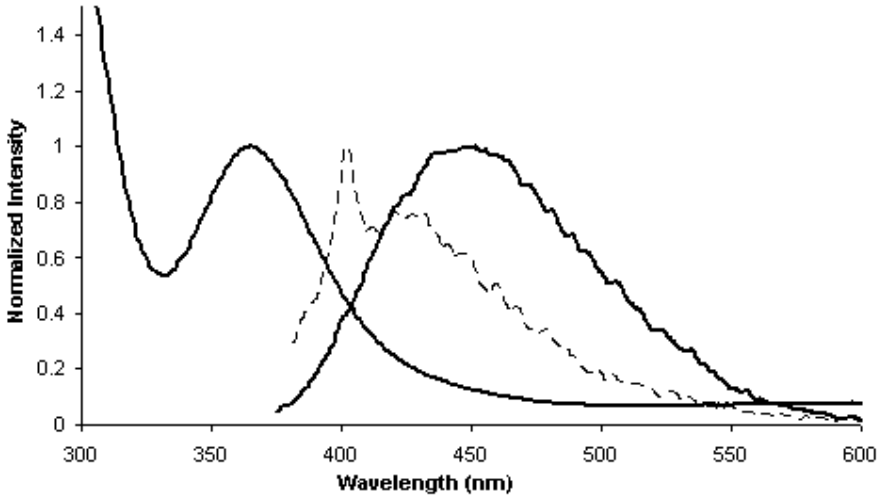

Fig. 6 – Absorption and emission spectra of TiS_2 nanoclusters, showing the absorption spectrum in octane (solid curve on left), emission spectrum in octane (solid curve on right) and the emission spectrum in acetonitrile (dotted curve) after excitation at 360 nm.

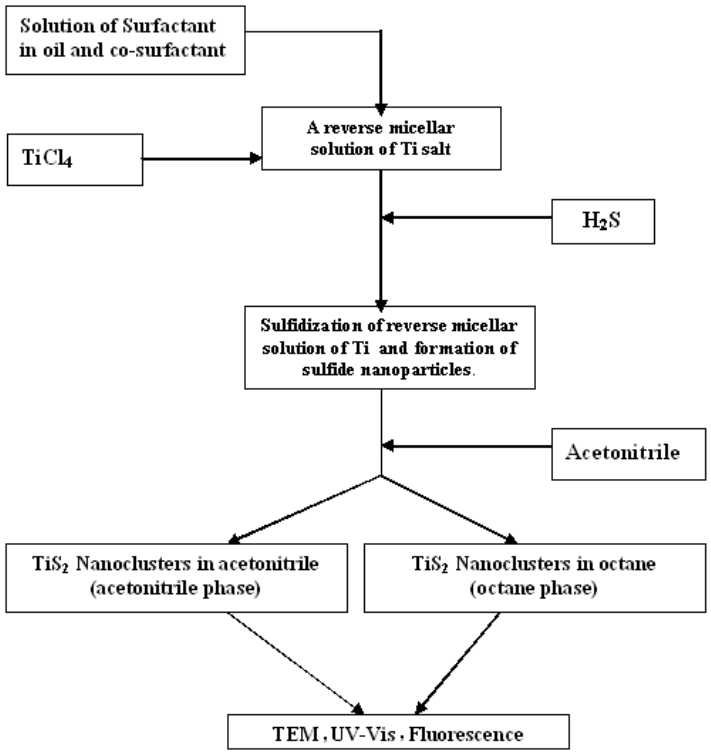

Fig. 7 – Scheme for TiS_2 nanoparticle synthesis using reverse micelles at room temperature.

In summary, we have successfully synthesized nano-size clusters of the layered semiconductor, TiS_2, at room temperature, and report their structural and optical characteristics. The large blue shift in the optical absorption spectrum with decreasing cluster size affords the potential to tailor band gaps. Significant photoluminescence is observed at room temperature, which is absent in the bulk material, demonstrating the crossover from solid-like to molecule-like optical absorption spectra as the size of the clusters becomes smaller than that of the exciton in the bulk. Nanocluster systems, such as the TiS_2 synthesized here, offer the possibility of optimizing solar absorbance by using systems with mixed size band-gaps and potentials.

EXPERIMENTAL

The flow scheme presented in Figure 7 outlines the experimental procedure adopted for the synthesis of titanium disulphide nanoparticles in reverse micelles. Titanium tetrachloride was dissolved in a degassed ternary mixture containing a surfactant (tridodecylmethyl ammonium iodide (TDAI)), hexanol and octane in a weight ratio of 8/8/84, to give an inverse micelle solution (typical sample volumes were 6 mL) at a concentration of 8×10^{-4} M $TiCl_4$. A steady stream of hydrogen sulfide (H_2S) gas was then bubbled through the solution at room temperature for 5 minutes, during which time the clear solution turned dark yellow but no solid was observed to form. Following H_2S addition, the mixture was allowed to stir for 2 hours to ensure complete reaction, then the TiS_2 nanoclusters were extracted with an equal volume of acetonitrile. This dissolved the inverse micelles, with the hexanol and TDAI entering the acetonitrile phase, whilst the nanoclusters distributed between both the nonpolar octane phase and the polar acetonitrile/TDAI/hexanol phase.

High-resolution transmission electron microscopy (HRTEM) using Philips CM 200 FEG microscope has been used to study the microstructure of particles. Fluorescence measurements were carried out on a Perkin-Elmer LS-50B.

Acknowledgements: The CRC for Microtechnology is acknowledged for financial support of the project, together with Ju Lin Peng for assistance with the HRTEM.

REFERENCES

1. Y.-S. Kim, M. Masataka, T. Isao and A. Hirohiko, *Material Transaction, JIM*, **1988**, *39*, 709 - 713.
2. R.C. Bill, *Wear,* **1985**, *106*, 283 – 289.
3. J. Chen, S.Li, Z.L. Tao, Y.T. Shen and C.X. Cui, *J.Am.Chem. Soc*., **2003**, *125*, 5284 – 5286.
4. H.W. Myron and A.J. Freeman, *Phys. Rev. B,* **1974**, *9*, 481.
5. T.J. Wieting and M. Schlűter, "Electrons and Phonons in Layered Crystal Structures", Reidel, Holland, 1979, p. 190-223.
6. A.R. Beal, J.C. Knights and W.Y.Liang, *J.Phys. C: Solid State Phys.,* **1972**, *5*, 3540 - 3547.
7. A.D. Yoffe, *Adv. Phys.,* **1993**, *42*, 173 – 209.
8. L.E. Brus, *J. Phys. Chem.,* **1986**, *90*, 2555 – 2563.
9. M.V. Rama and R.A. Friesner, *J. Chem. Phys.,* **1991**, 95, 8309 - 8315
10. P.E. Lippens and M. Lannoo, *Phys. Rev. B,* **1989**, *39*, 10935 – 10943.
11. J.M. Huang and D.F. Kelley, *J. Chem. Phys.,* **2000**,*113*, 793 – 797.
12. J.P. Wilcoxon, G. Samara, P. Newcomer, *Materials Research Society Symposium Proceedings*, **1995**, *358*, 277 - 283.
13. J.S. Huang, *J. Phys. Chem. B.*, **1985**, *82*, 480 - 487.
14. R. Doolen, R. Laitinen, F. Parsapour and D.F. Kelley, *J. Phys. Chem. B,* **1998,** 102, 3906 - 3913.
15. J.M. Huang, R.A. Laitinen and D.F. Kelley, *Phys. Rev. B*, **2000,** 62, 10995 - 11003.
16. J.M. Huang and D.F. Kelley, *J. Chem. Phys*, **2000,** 113, 793 - 799
17. J.P. Wilcoxon and G.A. Samara, *Phys. Rev. B*, **1995,** 51, 7299 – 7305.
18. F. Parsapour, D.F. Kelley, S. Craft and J. P. Wilcoxon, *J. Chem. Phys*. **1996,** 104, 4978 - 4983.
19. F. Parsapour, D.F. Kelley and R.S. Williams, *J. Phys. Chem. B*, **1998,** 102, 7971 - 7975.
20. A. Let PhD thesis, Royal Melbourne Institute of Technology, Melbourne.
21. J.P. Wilcoxon, G.A. Samara, D. Bliss and P. Newcomer, *Proceedings Electrochemical Society,* **1996,** *95-25*, 432 – 443.
22. L.E. Brus, *J. Chem. Phys,* **1983**, 79, 5566 - 5572.
23. L.E. Brus, *J. Chem. Phys*, **1984,** 80, 4403 - 4412.
24. L.E. Brus *J. Phys. Chem,* **1986,** 90 2555 - 2563
25. R. Rosetti, J.E. Ellison, J.M. Gibson and L.E. Brus, *J.Chem. Phys,* **1984**, 80, 4464 - 4472.
26. L.E. Oliveira, *Phys. Stat. Sol. B: Basic Research,* **1988,**147, 223 - 231.
27. H. Isomaki, J von Boehm and P. Krusius, *J. Phys.C: Solid State Physics,* **1979,** 12, 3239 - 3245.